

# Topological liquid nucleation induced by vortex-vortex interactions in Kitaev's honeycomb model

Ville Lahtinen<sup>1</sup>, Andreas W. W. Ludwig<sup>2</sup>, Jiannis K. Pachos<sup>3</sup>, and Simon Trebst<sup>4</sup>

<sup>1</sup>*NORDITA, Roslagstullsbacken 23, 106 91 Stockholm, Sweden*

<sup>2</sup>*Department of Physics, University of California, Santa Barbara, CA 93106, USA*

<sup>3</sup>*School of Physics and Astronomy, University of Leeds, LS2 9JT Leeds, UK and*

<sup>4</sup>*Microsoft Research, Station Q, University of California, Santa Barbara, CA 93106, USA*

(Dated: April 11, 2022)

We provide a microscopic understanding of the nucleation of topological quantum liquids for interacting non-Abelian anyons by making an explicit connection between the microscopics of the pairwise interactions – typically showing RKKY-type behavior oscillating in sign, but decaying exponentially with distance – and the nature of the collective many-anyon state. We investigate this issue in the context of Kitaev's honeycomb lattice model. For non-Abelian vortex excitations arranged on superlattices, we observe the nucleation of several distinct Abelian topological phases whose character is found to depend on microscopic parameters such as the vortex-spacing or the strength of the time-reversal symmetry breaking field. By reformulating the interacting vortex superlattice in terms of an effective model of Majorana fermion zero modes, we show that the collective behavior can be fully traced back to the pairwise vortex interactions. We find that longer-range interactions beyond nearest neighbor can influence the nature of the collective state and thus need to be included for a comprehensive picture. Corresponding results should hold for vortices forming an Abrikosov lattice in a  $p$ -wave superconductor or quasiholes forming a Wigner crystal in non-Abelian quantum Hall states.

*Introduction.*– One of the most intriguing aspects of a topological phase is the emergence of anyonic quasiparticles. If these obey non-Abelian statistics, their presence gives rise to a (macroscopic) ground state degeneracy, a distinctive feature which has been suggested to be exploited for topological quantum computation [1]. However, in any microscopic system this degeneracy will be lifted by the omnipresent interactions between the anyons. These interactions are often assumed to be extremely weak due to the localized nature of the anyon wavefunction, but their strength grows exponentially when the anyons are brought into proximity. In fact, they can reach sizable magnitude when the anyon separation becomes of the order of the characteristic length scale, such as the magnetic length in quantum Hall liquids [2], the coherence length in a  $p$ -wave superconductor [3], or the plaquette spacing in Kitaev's honeycomb model [4]. When such strongly interacting anyons form regular arrangements (e.g. a Wigner crystal or an Abrikosov lattice), it has been shown that the collective degeneracy is split, and a unique topological liquid (distinct from the parent state of which the anyons are excitations) is selected as the new ground state [5], a mechanism referred to as topological liquid *nucleation*. While it has been appreciated that the character of the nucleated topological liquid depends on the sign of the pairwise interactions, we expand this perspective in the manuscript at hand to include the microscopic effects of longer range interactions expected to play a role for dense arrangements of anyons. This provides a comprehensive understanding how nucleation occurs in microscopic situations.

As a prototypical system that allows good control of all microscopic parameters, we study nucleation in the context of Kitaev's honeycomb lattice model. It is an exactly solvable spin model [6] defined by the Hamiltonian

$$H = J \sum_{\gamma\text{-links}} J_{\gamma} \sigma_i^{\gamma} \sigma_j^{\gamma} + K \sum_{(i,j,k)} \sigma_i^x \sigma_j^y \sigma_k^z, \quad (1)$$

where the  $\sigma_i^{\gamma}$  denote the standard Pauli matrices describing spin-1/2 moments on the sites of the lattice,  $\gamma = x, y, z$  indicates the different link types of the lattice,  $J_{\gamma}$  are the strengths of the nearest neighbor spin exchange along these links and  $K$  is the magnitude of a three spin term that explicitly breaks time reversal symmetry. Our starting point is the well-studied non-Abelian topological phase occurring in the vicinity of isotropic spin exchange  $J_x = J_y = J_z$  and for a finite three-spin exchange  $K > 0$ . The elementary excitations in this topological phase are magnetic vortices [7] centered on the plaquettes of the honeycomb lattice that exhibit the non-Abelian statistics of Ising anyons [6]. Two such vortices can combine into two possible collective states whose corresponding energies sensitively depend on the separation of the two vortices [4], as illustrated in Fig. 1. Increasing the vortex separation  $d$ , the energy splitting  $\epsilon(d)$  between these two states is found to decay exponentially while showing RKKY-like sign oscillations. These features have also been found in the Moore-Read quantum Hall state [2] and  $p_x + ip_y$  superconductors [3], though the precise values for the amplitude and the frequency of the oscillations depend on the specific microscopic situation.

Using this microscopic input for the pair splitting we turn to the *many-vortex* problem and ask which collective ground state is formed as we arrange vortices in superlattices of equal spacing  $D = 1, 2, 3, \dots$  (in units of the plaquette lattice spacing, see Fig. 4). We are interested in varying the superlattice spacing  $D$  for two reasons. First, each vortex spacing tunes the pairwise interactions and the ratio of nearest and next-nearest neighbor interactions to different microscopic values, which we find to result in different collective states. Second, going through the sequence of possible superlattice spacings closely mimics the expansion of a Wigner crystal of quasiholes when shifting the magnetic field on a quantum Hall plateau, or similarly the expansion of an Abrikosov lattice of vortices in a  $p$ -wave superconductor when varying the applied

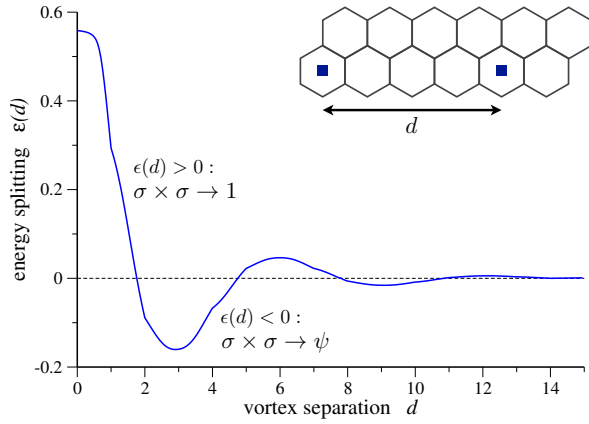


FIG. 1: Microscopics of the interaction between a pair of vortices in Kitaev’s honeycomb lattice model: The non-Abelian vortices can combine into two possible collective states according to the fusion rule  $\sigma \times \sigma = 1 + \psi$ . In general, these two states have energies  $E_1$  and  $E_\psi$ , with the splitting  $\epsilon(d) = E_\psi - E_1$  between them decreasing exponentially with vortex separation  $d$  and showing characteristic oscillation due to interference effects. When  $\epsilon(d) > 0$  ( $< 0$ ) the system energetically favours the state where the vortices combine into the trivial (fermionic) excitation.

magnetic field.

*Nucleated phases and vortex band structure.*— To determine the collective ground state in the presence of a vortex-superlattice, we follow Kitaev’s original analytical approach [6] and map the spin model (1) to a system of free Majorana fermions coupled to a  $Z_2$  gauge field. This also enables the exact (numerical) diagonalization of the system in the presence of an arbitrary vortex superlattice [8]. Our results are given in Fig. 2 where we plot the lowest gap in the energy spectrum (for a system with periodic boundary conditions) along a cut in the phase diagram parametrized by  $1/3 \leq J_z \leq 1/2$  and  $J_x = J_y$ . In the absence of vortices we observe a continuous phase transition at  $J_z = 1/2$  between the Abelian toric code (TC) phase for  $J_z > 1/2$  and the non-Abelian phase characterized by a Chern number  $\nu = -1$  for  $J_z < 1/2$ . In the presence of a vortex superlattice we again find a continuous phase transition (at which the respective energy gaps close), but which occurs now at some  $J_z^c$  separating the TC phase ( $J_z > J_z^c$ ) from a distinct *Abelian* topological phase for  $J_z < J_z^c$  (in lieu of the non-Abelian phase observed in the absence of a vortex superlattice), characterized by an even Chern number. The Chern number of this new Abelian phase is found to depend on the superlattice spacing with a sequence of  $\nu = -2, -4, 0$  observed for integer spacings  $D = 1, 2, 3$ , as shown in Fig. 2. The precise location  $J_z^c$  of the phase transition also depends on the superlattice spacing, with the common feature that the TC phase is always enlarged in the presence of a vortex superlattice, i.e.  $J_z^c < 1/2$ .

For each of the Abelian topological phases a further investigation of the energy spectrum reveals a characteristic band structure: For the full-vortex lattice ( $D = 1$ ) the spectrum, shown in Fig. 3, exhibits four gapped Dirac cones [9]. The

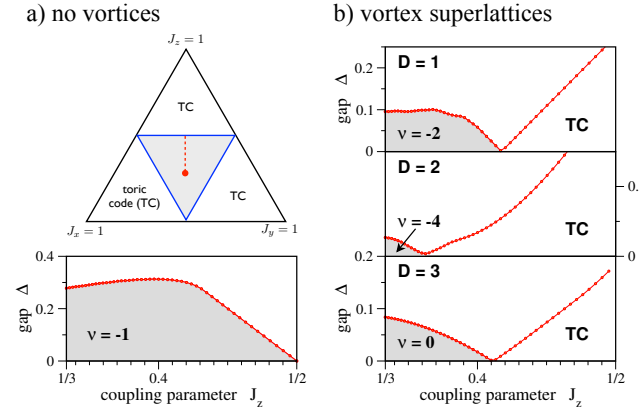


FIG. 2: (a) Phase diagram of the Kitaev model (1) parametrized by couplings  $\sum_\gamma J_\gamma = 1$  and  $K > 0$ . (b) Cuts through the phase diagram (along  $1/3 \leq J_z \leq 1/2$  and  $J_x = J_y$ , indicated by the dashed line in (a)) in the presence of vortex superlattices with spacing  $D$ . Shown are the lowest gap  $\Delta$  in the energy spectrum and the classification of the nucleated topological phases in terms of Chern numbers. All numerical data shown is for  $K = 0.08$ .

$D = 2$  superlattice spectrum also exhibits four gapped Fermi points, but with a significantly broader (quadratic) dispersion. The energy spectrum for the  $D = 3$  superlattice, however, does not show indications of Fermi points. Interestingly, this phase remains gapped even as the three-spin coupling  $K$  is tuned to zero, thus indicating that it is adiabatically connected to the previously observed [10] gapped phase, that emerges when a vortex superlattice is imposed on the *gapless* time-reversal symmetric spin liquid (for which  $K = 0$ ).

The common feature of all these observed band structures is that they consist of low-energy *vortex bands*  $\Psi_v^\pm$  and a set of high-energy *fermion bands*  $\Psi_f^\pm$  (see Fig. 3). In the presence of  $2N$  vortices the first contains  $N$  states that have support only on the sites near the vortices, while the latter contains the rest of the states that in general have support on all sites of the honeycomb lattice. For any finite  $K$  the vortex and fermion bands are separated in energy by a band gap  $\Delta_{vf}$ . Hence the Chern number characterizing the ground state, that consists of the fully occupied negative energy bands  $\Psi_v^-$  and  $\Psi_f^-$ , can be written as

$$\nu = \nu_v + \nu_f, \quad (2)$$

where  $\nu_v$  and  $\nu_f$  are the Chern numbers for the individual  $\Psi_v^-$  and  $\Psi_f^-$  bands, respectively. We observe that the first depends on the underlying vortex configuration, while the latter contributes always  $\nu_f = -1$  for  $K > 0$ . The nucleated phases can thus be viewed as comprising of two decoupled theories: a remnant of the non-Abelian phase living on the honeycomb lattice and an emergent theory living effectively on the vortex lattice.

*Effective Majorana model.*— We now turn to obtain a microscopic understanding that connects the characteristics of the emergent vortex band structure (and its Chern number) to the

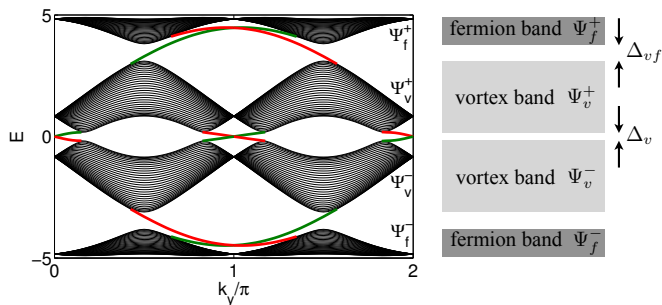


FIG. 3: The band structure of the nucleated topological phase (with Chern number  $\nu = -2$ ) for a  $D = 1$  vortex superlattice.  $\Psi_v^\pm$  ( $\Psi_f^\pm$ ) denote low-energy (high-energy) vortex (fermion) bands. For the periodic boundary conditions of a torus (black lines) the spectrum shows four gapped Dirac cones. For the open boundary conditions of a cylinder four edge modes (red and green lines) emanate from the gapped Dirac cones.

pairwise vortex interactions. The latter manifest themselves in the energy splitting shown in Fig. 1, but can also be viewed as arising from tunneling between Majorana fermion zero modes within the two vortex cores. In this spirit we formulate an effective lattice model of Majorana fermion zero modes tunneling on the vortex superlattice. To capture the interactions between vortex pairs separated by distances  $d = D, D\sqrt{3}$  (see Fig. 4), our model incorporates both nearest and next-nearest neighbor hopping (denoted by n.n. and n.n.n., respectively)

$$H = it_1 \sum_{\langle ij \rangle} s_{ij} \gamma_i \gamma_j + it_{\sqrt{3}} \sum_{\langle\langle ij \rangle\rangle} s_{ij} \gamma_i \gamma_j, \quad (3)$$

where the  $\gamma_i$  denote Majorana zero modes at vortex location  $i$  (the center of honeycomb plaquette) obeying  $\{\gamma_i, \gamma_j\} = 2\delta_{ij}$ . The microscopics of the vortex interactions (see Fig. 1) enter this model by identifying the amplitude of the nearest neighbor and next-nearest neighbor hopping,  $t_1$  and  $t_{\sqrt{3}}$ , with the energy splitting for a pair of vortices separated by the corresponding distance [11]. Finally, we note that the model allows for additional  $Z_2$  gauge choices  $s_{ij} = \pm 1$ , which need to be chosen in such a way that the fluxes per triangular plaquette with corners  $i, j, k$  is  $\Phi_{ijk} = -i \ln(is_{ij}s_{jk}s_{ki}) = \pm\pi/2$ . We will fix the  $s_{ij}$  in the following way: Let us first consider the fluxes through the three distinct triangular plaquettes spanned by the hopping terms  $t_1$  and  $t_{\sqrt{3}}$ . As illustrated in Fig. 4(b) there are triangles spanned solely by either  $t_1$ - or  $t_{\sqrt{3}}$ -links, and those consisting of both. We denote the former as  $T_1$  and  $T_{\sqrt{3}}$ , respectively, and the latter as  $T_{1,\sqrt{3}}$ . It has been shown [13] that for  $t_{\sqrt{3}} = 0$  one obtains a gapped energy spectrum if one uniformly imposes a  $+\pi/2$ -flux or  $-\pi/2$ -flux on all triangles  $T_1$ . In the following we will fix this flux to be  $\Phi_{T_1} = +\pi/2$ . Extending this argument to the triangles  $T_{\sqrt{3}}$  and  $T_{1,\sqrt{3}}$ , which involve the  $t_{\sqrt{3}}$  hopping, we fix the fluxes on the respective triangles to be  $\Phi_{T_{\sqrt{3}}} = 3\pi/2 = -\pi/2 \pmod{2\pi}$  and  $\Phi_{T_{1,\sqrt{3}}} = +\pi/2$  such that the flux through a triangle is proportional to its enclosed area. Picking a periodic pattern of gauge choices  $s_{ij}$  satisfying these flux assignments, requires

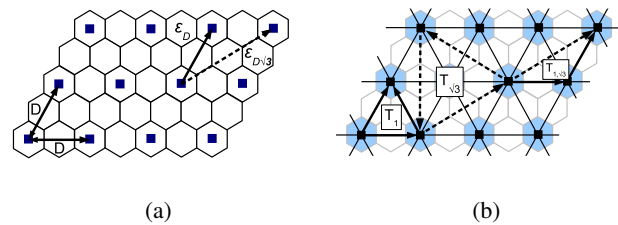


FIG. 4: (a) A vortex (blue squares) superlattice of spacing  $D$  (here  $D = 2$ ). (b) The effective model in terms of Majorana fermion zero modes tunneling on the triangular superlattice with hopping amplitudes  $t_1$  ( $t_{\sqrt{3}}$ ) indicated by the solid (dashed) lines. Their strengths are identified with the energy splittings  $\epsilon(d = D)$  and  $\epsilon(d = D\sqrt{3})$  at the corresponding separations. The fluxes in the effective model are chosen such that plaquettes indicated as  $T_1, T_{\sqrt{3}}$ , and  $T_{1,\sqrt{3}}$  enclose flux  $\Phi_{T_1} = \frac{\pi}{2}$ ,  $\Phi_{T_{\sqrt{3}}} = -\frac{\pi}{2}$ , and  $\Phi_{T_{1,\sqrt{3}}} = \frac{\pi}{2}$ , respectively.

a unit cell of at least 36 sites.

We (numerically) diagonalize this effective mode for varying relative amplitudes of the two hopping terms  $t_1, t_{\sqrt{3}}$  by parametrizing  $t_1 = \cos\theta$  and  $t_{\sqrt{3}} = \sin\theta$  (up to an overall common scale). Independent of the relative coupling we find that our effective model gives rise to a gapped band structure with Chern numbers  $\nu_v = \pm 1, \pm 3$  as indicated in the phase diagram of Fig. 5. The occurrence of some of these particular Chern numbers can be readily understood in the following way: If the nearest-neighbor hopping dominates ( $t_1 \gg t_{\sqrt{3}}$ ) then we recover the analytically tractable triangular lattice problem studied before [13], which has been shown to give  $\nu_v = \pm 1$  where the sign corresponds to the sign of  $t_1$ . Similarly, in the opposite limit  $t_{\sqrt{3}} \gg t_1$  the system simply decomposes into three uncoupled copies of the triangular lattice problem, thus giving a Chern number of  $\nu_v = \pm 3$ . Finally, there is an intermediate phase with Chern number  $\nu_v = \mp 3$  arising for  $t_1 \approx -t_{\sqrt{3}}$ .

Equipped with these quantitative results for the effective Majorana model (3) we can now return to the original system of interacting vortices in Kitaev's spin model (1) and look whether these results now allow us to establish a direct connection between the microscopic energy splitting for a vortex pair and the observed collective ground state in the presence of a vortex superlattice. Indeed such a connection can be established for various superlattice spacings  $D$  and varying the three-spin interaction  $K$ , while (for simplicity) assuming isotropic spin exchange  $J_x = J_y = J_z$  in (1). Keeping in mind that the Chern number for the topological phases in the original Kitaev model includes the contribution (2) from the fermion band  $\nu = \nu_v - 1$ , we find matching results for vortex superlattices with spacing  $1 < D \leq 6$ , i.e. the vortices are well separated. As illustrated in Fig. 6 for superlattice spacings  $D = 2$  and  $D = 3$  the observed sequence of phases with Chern numbers  $\nu = 0, \pm 2, -4$  as a function of the three-spin term  $K$  is in *quantitative* agreement with our microscopic approach. For denser vortex lattices, in particular the fully packed vortex lattice with  $D = 1$ , we find agree-

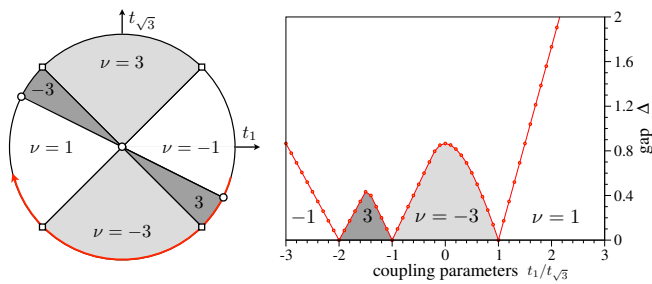


FIG. 5: (a) The phase diagram of the effective Majorana fermion zero mode model (we parametrize here  $t_1 = \cos \theta$  and  $t_{\sqrt{3}} = \sin \theta$ ), as characterized by the Chern numbers  $\nu_v$ , for the flux assignment  $(\Phi_{T_1}, \Phi_{T_{\sqrt{3}}}, \Phi_{1, T_{\sqrt{3}}}) = (\frac{\pi}{2}, -\frac{\pi}{2}, \frac{\pi}{2})$ . The squares and the circles denote phase transitions at  $|t_1| = |t_{\sqrt{3}}|$  and  $t_1 = -2t_{\sqrt{3}}$ , respectively. (b) The lowest gap in the energy spectrum,  $\Delta_v$ , along the path shown in (a) for  $t_{\sqrt{3}} = -1$ .

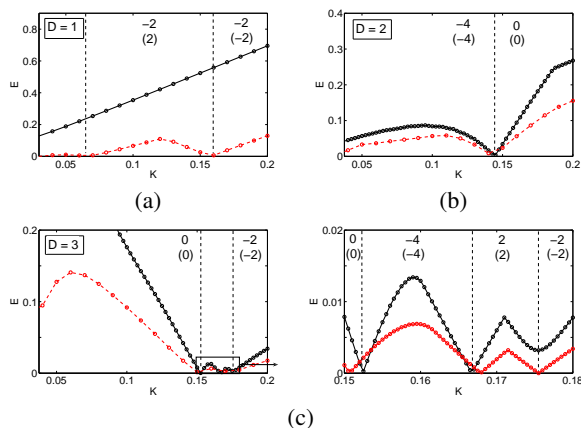


FIG. 6: The energy gaps  $\Delta$  of the nucleated phases in the honeycomb model (solid black lines) and the gap  $\Delta_v$  predicted by the effective model (dashed red lines) for (a)  $D = 1$ , (b)  $D = 2$  and (c)  $D = 3$  vortex superlattices. The numbers without (with) parenthesis are the Chern numbers  $\nu$  ( $\nu_v - 1$ ) of the nucleated phases (predicted from the interactions). The right plot in (c) is a zoom of the region  $0.15 < K < 0.18$  for the  $D = 3$  superlattice. Note the quantitative similarity of the sequence of phases to that of Fig. 5.

ment only in the limit of large three-spin exchange  $K \gtrsim 0.15$ . For smaller three-spin exchange, presumably the coherence length increases (as the gap decreases) beyond the spacing of the fully packed vortex configuration, thus rendering the notion of individual vortices on these plaquettes poorly defined and therefore making our microscopic approach inapplicable.

*Conclusions.*— To summarize, we have studied in microscopic detail the nucleation of topological liquids arising due to vortex-vortex interactions in Kitaev’s honeycomb model, which we consider a prototypical system allowing for good control of the microscopic vortex interactions. Considering longer ranged vortex-vortex interactions going beyond the nearest neighbor exchange, we could make a direct connection between the microscopic input for the sign, amplitude and ratio of the pairwise couplings to the observed collective

many-vortex state via an effective model in terms of Majorana fermion zero modes (and longer-ranged hopping terms). Generally, we find that vortex-vortex interactions destroy the non-Abelian nature of the underlying topological phase and nucleate an Abelian topological phase, whose band structure and Chern number description sensitively depends on the microscopics of the vortex-vortex interactions, such as the spacing of the vortex superlattice or the strength of the time-reversal symmetry breaking term  $K$ . In particular, we reported the occurrence of Abelian phases with Chern numbers  $\nu = +2$  or  $\nu = -4$ , which arise when next-nearest neighbor interactions become of comparable magnitude as the nearest-neighbor interactions (but have different signs). Our results should also be of direct relevance to the physics of non-Abelian quantum Hall states, where detuning the magnetic field away from the middle of the plateau will have the effect of contracting the spacing of the Wigner crystal formed by quasihole excitations, and similarly applies to Abrikosov lattices of vortices in  $p$ -wave superconductors. Further studies will address the microscopics of a recently observed thermal metal state [14] for non-Abelian vortices with random exchange.

*Acknowledgments.*— This work has been supported, in part, by the Finnish Academy of Science (V.L), the NSF (A.W.W. L.) through DMR-0706140, and the Royal Society (J.P.), V.L. would like to thank G. Kells for insightful discussions.

- [1] A. Kitaev, *Ann. Phys.* **303**, 2 (2003) and quant-ph/9707021; for a more recent discussion see also C. Nayak *et al.*, *Rev. Mod. Phys.* **80**, 3 (2008); see *e.g.* also G.K. Brennen and J.K. Pachos, *Proc. R. Soc. A* **464**, 1 (2008).
- [2] M. Baraban *et al.*, *Phys. Rev. Lett.* **103**, 076801 (2009).
- [3] M. Cheng *et al.*, *Phys. Rev. Lett.* **103**, 107001 (2009).
- [4] V. Lahtinen, *New J. Phys.* **13**, 075009 (2011).
- [5] C. Gils *et al.*, *Phys. Rev. Lett.* **103**, 070401 (2009); A.W.W. Ludwig *et al.*, *New J. Phys.* **13**, 045014 (2011).
- [6] A.Y. Kitaev, *Ann. Phys.* **321**, 2 (2006).
- [7] For a system of  $2N$  spins Hamiltonian (1) has  $N$  local symmetries  $[H, \hat{W}_p] = 0$ , where  $\hat{W}_p$  are mutually commuting  $\mathbb{Z}_2$  valued six-spin operators associated with every plaquette  $p$ . Their eigenvalues  $w_p = -1$  denote a  $\pi$ -flux vortex at plaquette  $p$ , while  $w_p = 1$  denotes an absence of one [6].
- [8] V. Lahtinen *et al.*, *Ann. Phys.* **323**, 2286 (2008).
- [9] V. Lahtinen and J.K. Pachos, *Phys. Rev. B* **81**, 245132 (2010); J. K. Pachos, *Ann. Phys.* **322**, 1254 (2007).
- [10] M. Kamfor *et al.*, *Phys. Rev. B* **84**, 153404 (2011).
- [11] The sign of the energy splitting is only defined with respect to the overall fermionic parity  $P_d$  of a given vortex sector [12]. For the effective model corresponding to a superlattice of spacing  $D$ , we use thus the hopping amplitudes ansatz  $t_d = (-1)^{P_d D} |\epsilon(dD)|$ , where  $P_d = 0$  (1) for even (odd) fermionic parity. The energy splittings  $|\epsilon(D)|$  can be read directly from Fig. 1, but for  $|\epsilon(D\sqrt{3})|$  one has to carry out separate studies for the appropriate two vortex configurations.
- [12] G. Kells, J.K. Slingerland, and J. Vala, *Phys. Rev. B* **80**, 125415 (2009); F. Pedrocchi, S. Chesi, and D. Loss, *Phys. Rev. B* **84**, 165414 (2011).
- [13] E. Grosfeld and A. Stern, *Phys. Rev. B* **73**, 201303 (2006).

[14] C.R. Laumann *et al.*, arXiv:1106.6265